J. Austral. Math. Soc. Ser. B 36(1994), 1–16

ANALYSIS OF A DIFFERENTIAL EQUATION OCCURRING IN THE THEORY OF FLAME FRONTS

R. GRIMSHAW and J. GAN[1]

(Received 20 July 1992; revised 26 March 1993)

Abstract

Ronney and Sivashinsky [2] and Buckmaster and Lee [1] have proposed a certain non-autonomous first order ordinary differential equation as a simple model for an expanding spherical flame front in a zero-gravity environment. Here we supplement their preliminary numerical calculations with some analysis and further numerical work. The results show that the solutions either correspond to quenching, or to steady flame front propagation, or to rapid expansion of the flame front, depending on two control parameters. A crucial component of our analysis is the construction of a barrier orbit which divides the phase plane into two parts. The location of this barrier orbit then determines the fate of orbits in the phase plane.

1. Introduction

Our purpose in this paper is to describe some analytical and numerical results for the following autonomous system of ordinary differential equations,

$$\frac{dR}{dt} = \psi, \tag{1a}$$

$$\frac{d\psi}{dt} = \frac{2\psi^2}{R} - L\psi + \psi^3\left(\tfrac{1}{3}kR^3 - \ln\psi\right), \tag{1b}$$

where t is a (scaled) time variable, the dependent variables are ψ, R and L, k are parameters. Eliminating t, we obtain a first-order non-autonomous equation for $\psi(R)$,

$$\frac{d\psi}{dR} = \frac{2\psi}{R} - L + \psi^2\left(\tfrac{1}{3}kR^3 - \ln\psi\right). \tag{2}$$

Equations (1a, b), or (2), were introduced by Ronney and Sivashinsky [2] for the case $k = 0$ as a simple model of an expanding spherical flame front in a zero-gravity

[1]Department of Mathematics, Monash University, Clayton, Vic. 3168, Australia.

https://doi.org/10.1017/S0334270000010195 Published online by Cambridge University Press

environment. In this context R is the (scaled) flame front radius, and ψ is the (scaled) flame front speed, while L is a parameter representing heat loss effects. Hence we shall confine our discussion to the situation when $\psi, R > 0$ and $L \geq 0$. Ronney and Sivashinsky [2] showed by some numerical calculations that, depending on the value of L, the solutions of (2) for the case $k = 0$ either correspond to quenching ($\psi \to 0, R \to R_0$ as $t \to \infty$ with $0 < R_0 < \infty$), or to steady flame front propagation ($\psi \to \psi_0, R \to \infty$ as $t \to \infty$ where $0 < \psi_0 < \infty$).

However, experimental observations show that the quenching radius R_0 may be very sensitive to the initial conditions of the experiment, a feature not captured by the model equation (2) when $k = 0$. Hence Buckmaster and Lee [1] introduced the term with coefficient $k > 0$ into (2) in an attempt to explain this phenomenon, and showed by some numerical calculations that for $k > 0$ it is possible for some solutions of (2) to exhibit quenching, while solutions with nearby initial conditions show divergence ($R, \psi \to \infty$). Here the new term models the effects of confinement (i.e., finite chamber volume) and k is a confinement parameter. The main physical effect of confinement is a pressure rise giving a non-local effect on the flame front.

In this paper we explore the parameter space $k, L \geq 0$ for the solutions of (2). It is not our purpose to provide a detailed physical interpretation of the results, or a discussion of the validity of (2) as a model for spherical flame fronts, and we refer the reader to Ronney and Sivashinsky [2] or Buckmaster and Lee [1] for these aspects. However, we are guided by the underlying physics in our analysis, and hence the primary aim is to determine when quenching occurs, as opposed to the alternatives of steady flame front propagation or an expanding flame ($R, \psi \to \infty$). Although we are mainly concerned with the case $k > 0$, we shall in Section 2 describe in detail the situation for $k = 0$ as this provides a suitable framework for the situation when $k > 0$ but quite small. Then in Section 3 we discuss the case the $k > 0$, concentrating on small values of k. We shall show that the solutions do exhibit some sensitivity, both to the initial conditions and to the value of k. However, we should point out immediately that because (1a, b) is an autonomous system of the second order there is no possibility here of chaotic behaviour.

2. The case k=0

First we seek steady states for which $\psi = \psi_0$ where ψ_0 is a constant. The first possibility is that $\psi_0 = 0$, in which case $R = R_0$ where R_0 is a non-zero, finite constant. This corresponds to quenching, and is a stable state; $\psi \to 0$ and $r \to R_0$ as $t \to \infty$. If $\psi_0 > 0$, then $R \to \infty$ as $t \to \infty$ and corresponds to a front with constant speed. From (1b) or (2), ψ_0 is given by

$$L + \psi_0^2 \ln \psi_0 = 0. \tag{3}$$

https://doi.org/10.1017/S0334270000010195 Published online by Cambridge University Press

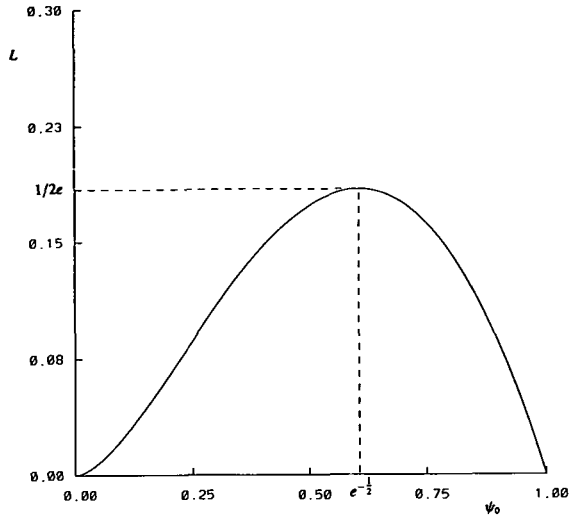

FIGURE 1. A plot of the steady states when $k = 0$, given by (3).

This is plotted in Figure 1. There are two solutions for $0 \leq L < L_0$, where $L_0 = 1/2e$, denoted by $\psi_0^{\pm}$. It is readily shown that the upper branch ψ_0^+ is stable, and the lower branch ψ_0^- is unstable, where $0 \leq \psi_0^- < e^{-\frac{1}{2}} < \psi_0^+ \leq 1$.

Next we examine the turning-point curve, defined as the curve on which $d\psi/dR = 0$. From (2), it is given by

$$R = \frac{2\psi}{L + \psi^2 \ln \psi}. \tag{4}$$

We plot this curve in Figure 2. In Figure 2(a), $0 < L < L_0$ and we see that the turning-point curve has two branches each with an asymptote $\psi \to \psi_0^{\pm}$ as $R \to \infty$. In Figure 2(b), $L > L_0$ and we see that the turning-point curve has a single branch. In both cases (a) and (b)

$$R \sim \frac{2}{\psi \ln \psi} \quad \text{as} \quad \psi \to \infty, \tag{5a}$$

and

$$R \sim 2\psi/L \quad \text{as} \quad \psi \to 0. \tag{5b}$$

Also, it is readily shown from (2) that $\dfrac{d^2\psi}{dR^2}$ is negative when $\dfrac{d\psi}{dR} = 0$, so that solutions can only cross the turning-point curve from the region where $\dfrac{d\psi}{dR} > 0$ to the region where $\dfrac{d\psi}{dR} < 0$, i.e., from left to right.

Near R, $\psi \to 0$, we can deduce from (2) that

$$\psi = LR + AR^2 + O(R^3 \ln R). \tag{6}$$

https://doi.org/10.1017/S0334270000010195 Published online by Cambridge University Press

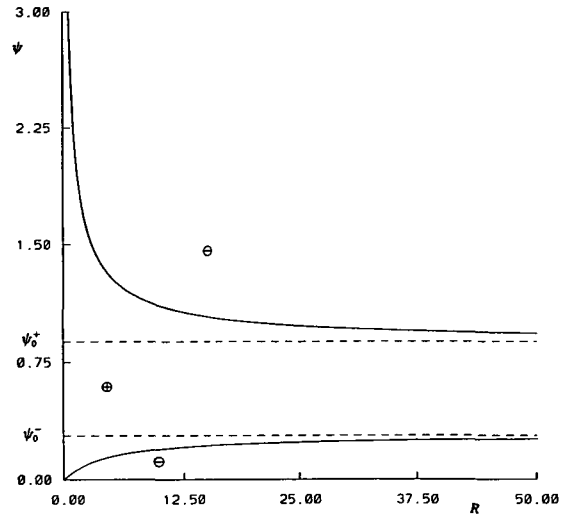

(a)

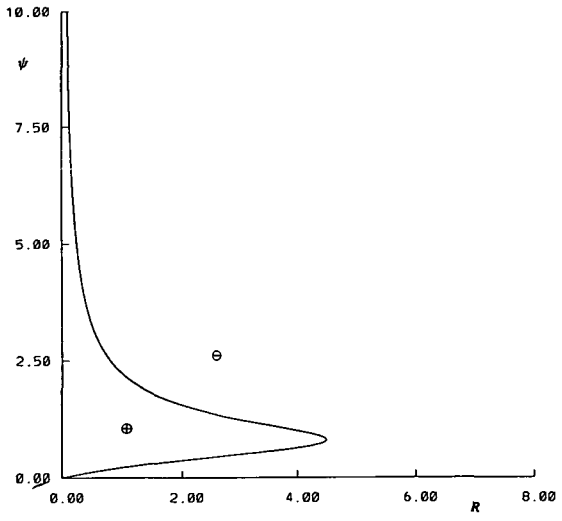

(b)

FIGURE 2. A plot of the turning-point curve when $k = 0$, given by (4), for (a) $L = 0.1 (0 < L < L_0)$ and (b) $L = 0.5 (L > L_0)$. Here $\psi_0^{\pm}$ are the steady states which exist in case (a), and $\oplus$ and $\ominus$ denote the regions where $d\psi/dR > 0$ or < 0 respectively.

Here A is an arbitrary constant, which can serve as a parameter to define a family of solutions emerging from the origin. Note that from (6) $R \sim \psi/L$ as $\psi \to 0$; comparing this with (5b) we see that all solutions emerging from the origin do so into the region $\dfrac{d\psi}{dR} > 0$. Then for $0 < L < L_0$ we can deduce that there is a critical value of A, A_c, such that for $A > A_c$, the orbit emerges from the origin, crosses

https://doi.org/10.1017/S0334270000010195 Published online by Cambridge University Press

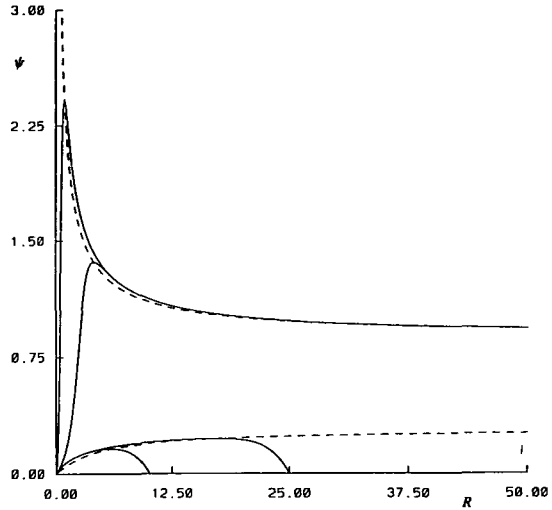

FIGURE 3. Typical orbits when $k = 0$ and $L = 0.1$, for the case $0 < L < L_0$. The dashed curves are the turning-point curves.

the upper branch of the turning-point curve (4) and then $\psi \to \psi_0^+$ as $R \to \infty$. For $A < A_c$, the orbit emerges from the origin, crosses the lower branch of the turning-point curve (4) and then $\psi \to 0$, $R \to R_0$. Here R_0 varies over the range $0 < R_0 < \infty$ with $R_0 \to \infty$ as $A \to A_c$ from below. These conclusions are based on local continuity with respect to the parameter A, and the observation that as $\psi \to \psi_0^+$, $\psi - \psi_0^+ \sim \left\{\left(\frac{1}{2} + \ln \psi_0^+\right) R\right\}^{-1}$ and hence the orbits which approach ψ_0^+ do so from above. Figure 3 shows some typical orbits.

However, for $L > L_0$, we can deduce that all orbits emerging from the origin will cross the turning-point curve (4) and as $t \to \infty$, $\psi \to 0$, $R \to R_0$. But here R_0 varies over the range $0 < R_0 < R_c$ with $R_0 \to R_c$ as $A \to \infty$. Thus all orbits emerging from the origin are quenched. Crucial to this conclusion is the establishment of the existence of a unique orbit for which $\psi \to \infty$ as $R \to 0$, which we shall call the barrier orbit (see Figure 4). We shall show that this barrier orbit lies always in the region $d\psi/dR < 0$, and its intersection with $\psi = 0$ then defines R_c. Then all orbits emerging from the origin are confined to the left of the barrier orbit. Orbits which lie to the right of the barrier orbit are such that $\psi \to \infty$ as $R \to R_1+$, and $\psi \to 0$ as $R \to R_0-$ where $R_0 > R_c$ and $R_1 > 0$. Some typical orbits are sketched in Figure 4.

To establish the existence of the barrier orbit, we suppose that $\psi \to \infty$ and $R \to 0$ simultaneously. Then we introduce the transformations

$$y = \ln \psi, \qquad f(y) = R\psi \tag{7}$$

https://doi.org/10.1017/S0334270000010195 Published online by Cambridge University Press

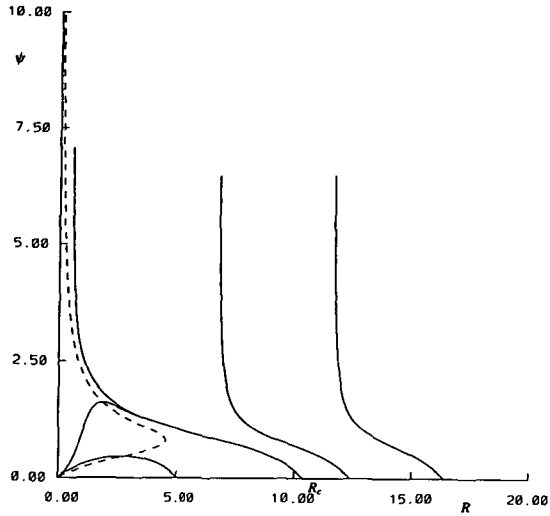

FIGURE 4. Typical orbits when $k = 0$ and $L = 0.5$, for the case $L > L_0$. The dashed curve is the turning-point curve.

and form a differential equation for $f(y)$ from (2).

$$\frac{df}{dy} = f\left\{1 + \left[2 - f\left(y + Le^{-2y}\right)\right]^{-1}\right\}. \tag{8}$$

In the limit $y \to \infty$, we seek a solution for which $yf \to$ constant. Some elementary analysis shows that if such a solution exists, then $yf \to 3$. To keep the analysis simple, we next note that the term Le^{-2y} is exponentially small in this limit, and can be neglected. Letting

$$g = yf \tag{9}$$

and omitting the term Le^{-2y} in (8) we get

$$\frac{dg}{dy} = g\left\{\frac{1}{y} - \frac{(3-g)}{(g-2)}\right\}. \tag{10}$$

Our aim now is to show that (10) has a unique solution such that $g \to 3$ as $y \to \infty$. It is sufficient here to consider $g > 2$ and $y > y_0 > 0$. Note that $dg/dy \to -\infty$ as $g \to 2$ from above, where $g = 2$ is the approximation to the turning-point curve (4) as $\psi \to \infty$. Next we note that $dg/dy = 0$ on the curve

$$g = 3 - 1/(y+1), \tag{11}$$

where $dg/dy > 0$ (< 0) above (below) this curve. Next we calculate

$$\frac{d^2g}{dy^2} = \frac{g\Delta}{y(g-2)^3}, \tag{12a}$$

https://doi.org/10.1017/S0334270000010195 Published online by Cambridge University Press

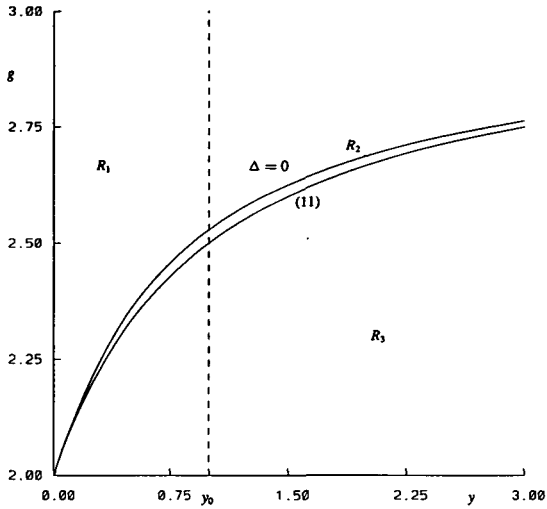

FIGURE 5. A plot of the turning-point curve (11) and $\Delta = 0$ (12b).

where

$$\Delta = y(g-3)(g^2-4g+6) + (g-2)(2g^2-9g+16). \tag{12b}$$

Then we can show that the curve $\Delta = 0$ passes through the point $y = 0$, $g = 2$, and for $y > 0$, always lies above the turning-point curve (11), while $g \to 3$ as $y \to \infty$. The situation is sketched in Figure 5, where we allow the curve (11) and $\Delta = 0$ to divide the region $y > 0$, $g > 2$ into 3 subregions, R_1, R_2 and R_3. Here R_1 is the region where d^2g/dy^2 and dg/dy are positive, R_2 is the region where d^2g/dy^2 is negative but dg/dy is positive, and R_3 is the region where d^2g/dy^2 and dg/dy are both negative. Further, we can show that dg/dy evaluated on $\Delta = 0$ is greater than the slope of $\Delta = 0$. It follows that orbits reaching $\Delta = 0$ must cross from R_2 into R_1. Similarly, orbits reaching the turning-point curve (11) must cross from R_2 into R_3. Consider now orbits commencing at $y = y_0 > 0$, with $g = g_0 > 2$. When (y_0, g_0) lies in R_1, the orbit proceeds upwards crossing $g = 3$ at a finite value of y. When (y_0, g_0) lies in R_3 the orbit proceeds downwards crossing $g = 2$ at a finite value of y. Next, when (y_0, g_0) lies in R_2, orbits starting close to $\Delta = 0$ will cross into R_1 while orbits starting close to the turning-point curve (11) will cross into R_3. By continuity with respect to g_0, there exists an orbit which remains in R_2 for all $y \geq y_0$.

To show that this orbit is unique, we first note that it is sandwiched between the curves (11) and $\Delta = 0$ as $y \to \infty$. Since (11) can be written in the form

$$\frac{1}{y} = \sum_{1}^{\infty} (3-g)^n, \tag{13}$$

https://doi.org/10.1017/S0334270000010195 Published online by Cambridge University Press

while $\Delta = 0$ has the expansion

$$\frac{1}{y} = \sum_{1}^{\infty} \alpha_n (3-g)^n, \tag{14a}$$

where

$$\alpha_1 = 1, \alpha_2 = \tfrac{4}{3}, \alpha_3 = \tfrac{4}{3}, \alpha_4 = \tfrac{10}{9}, \ldots, \tag{14b}$$

it follows that y^{-1} is $O(3-g)$ for this orbit, and indeed must have the expansion

$$\frac{1}{y} = \sum_{1}^{\infty} \beta_n (3-g)^n, \tag{15}$$

where clearly $\beta_1 = 1$, $1 < \beta_2 < \frac{4}{3}$ and so on. It follows that if (10) is written in the form

$$\frac{dg}{dy} = F(y, g), \tag{16}$$

then F is $O(y^{-2})$ as $y \to \infty$. Hence, we can integrate (16) to get

$$g = 3 + \int_{\infty}^{y} F(y', g(y'))\, dy'. \tag{17}$$

Standard iterative procedures can now be used on (17) to establish the existence of a unique solution. Finally we find that $\beta_2 = \frac{4}{3}$, $\beta_3 = \frac{10}{9}$ in (15).

This barrier orbit defines R_c (see Figure 4), where R_c depends on L, although we note from the analysis in the preceding two paragraphs that the asymptotic behaviour as $\psi \to \infty$, $R \to 0$ for the barrier orbit is given by

$$R \sim \frac{3}{\psi \ln \psi} - \frac{1}{\psi (\ln \psi)^2} + O\left(\frac{1}{\psi (\ln \psi)^3}\right), \quad \text{as } \psi \to \infty, \tag{18}$$

independently of L. Indeed there exists a unique solution with this asymptotic behaviour for all $L > 0$, but only for $L > L_0$ will this barrier orbit continue down to $\psi \to 0$, where $R \to R_c$. There is no obvious way to determine the dependence of R_c on L analytically, and so instead we do so numerically. We find that R_c decreases as L increases, and clearly $R_c \to \infty$ as $L \to L_0$ from above. In Table 1 we show some numerical results for R_c.

https://doi.org/10.1017/S0334270000010195 Published online by Cambridge University Press

L	R_c
0.3	22.964
0.5	10.3712
0.7	7.1055
0.9	5.5458

TABLE 1. The values of R_c in terms of L for $k = 0$.

3. The case k>0

With $k > 0$ we first note that there are now no steady states $\psi_0 > 0$, although $\psi \to 0$, and $R \to R_0$ remains a stable state corresponding to quenching. Next we consider the turning-point curve on which $\dfrac{d\psi}{dR} = 0$. This is here defined implicitly by

$$R = \frac{2\psi}{L + \psi^2 \ln \psi - \frac{1}{3}kR^3\psi^2}. \tag{19}$$

For all $k > 0$, this curve now has two branches. For $0 < k < k_c$ one branch is similar to the case $k = 0$ (see Figure 2(b)) and connects the limits $\psi \to \infty$, $R \to 0$ with the asymptotic behaviour (5a) to the limit $\psi \to 0$, $R \to 0$ with the asymptotic behaviour (5b). The second branch connects the limit $\psi \to \infty$, $R \to \infty$ to the limit $\psi \to 0$, $R \to \infty$ with the corresponding asymptotic behaviour

$$\tfrac{1}{3}kR^3 \sim \ln \psi, \quad \text{as} \quad \psi \to \infty, \tag{20a}$$

or

$$\tfrac{1}{3}kR^3 \sim L\psi^{-2}, \quad \text{as} \quad \psi \to 0. \tag{20b}$$

The situation is sketched in Figure 6(a). For $k > k_c$ the connection points for the branches interchange; see Figure 6(b). One branch now connects the limits $\psi \to \infty$, $R \to 0$ with the limit $\psi \to \infty$, $R \to \infty$ with the corresponding asymptotic behaviour (5a) and (20a) respectively. The other branch connects the limits $\psi \to 0$, $R \to 0$ with the limit $\psi \to 0$, $R \to \infty$ with the corresponding asymptotic behaviour (5b) and (20b) respectively. Further, for $0 < L < L_0$, we note that only case (b) can occur, and thus effectively $k_c = 0$; in particular the region $\psi_0^- < \psi < \psi_0^+$ lies between the two branches in the region where $d\psi/dR > 0$, where here we recall that $\psi_0^{\pm}$ are the solutions of (3) and are the steady states when $k = 0$. For $L > L_0$ both cases can occur with k_c a function of L. Here k_c can be determined by eliminating ψ, R from

https://doi.org/10.1017/S0334270000010195 Published online by Cambridge University Press

(a)

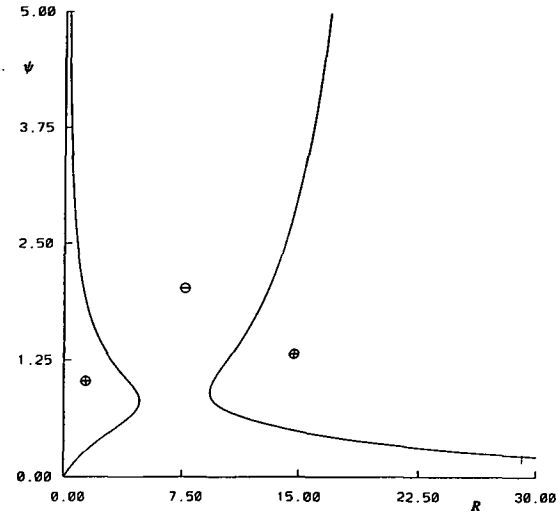

(b)

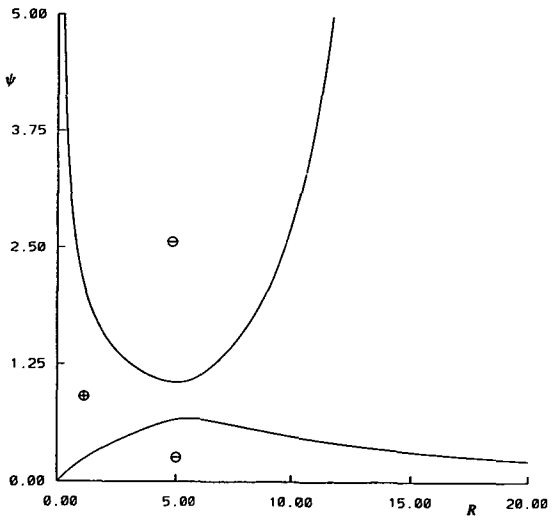

FIGURE 6. A plot of the turning-point curve (19) for $L = 0.5$ and (a) $k = 0.001$ ($0 < k < k_c$), (b) $k = 0.003$ ($k > k_c$). Here $\oplus$ and $\ominus$ denote the regions where $d\psi/dR > 0$ or < 0 respectively.

the following three equations

$$L + \psi^2 \ln \psi = \frac{2\psi}{R} + \tfrac{1}{3} k_c \psi^2 R^3, \tag{21a}$$

$$k_c \psi R^4 = 2, \tag{21b}$$

and

$$2\psi \ln \psi + \psi = \frac{2}{R} + \frac{2}{3} k_c \psi R^3. \tag{21c}$$

https://doi.org/10.1017/S0334270000010195 Published online by Cambridge University Press

L	k_c
0.3	0.000057
0.5	0.00192
0.7	0.00935
0.9	0.02565

TABLE 2. The values of k_c in terms of L, given by (22a, b).

Here (21a) is just (19) rewritten, while (21b) and (21c) are obtained by equating to zero the R- and ψ-derivatives of (21a) respectively. Eliminating R between these equations, we find that

$$k_c = \frac{2}{\psi}\left\{\frac{3\psi}{10}(2\ln\psi + 1)\right\}^4, \tag{22a}$$

where

$$\psi^2\left(\tfrac{3}{5}\ln\psi + \tfrac{4}{5}\right) = L. \tag{22b}$$

This pair of equations gives k_c parametrically as a function of L. It is readily shown from (22a, b) that k_c increases with L. Some typical values are shown in Table 2; note that k_c is generally quite small, and that $k_c \to 0$ as $L \to L_0$.

We are now in a position to describe the orbits in the positive quadrant of the $\psi - R$ plane. First we note that as $R, \psi \to 0$ the orbits are again described by (6), and hence there is a one–parameter family of solutions emerging from the origin into a region where $d\psi/dR > 0$. Next we again consider the existence of an orbit such that $\psi \to \infty$ as $R \to 0$. Using the transformation (7) we now get, in place of (8),

$$\frac{df}{dy} = f\left\{1 + \left[2 - f/y + Le^{-2y} - \tfrac{1}{3}kf^3e^{-3y}\right]^{-1}\right\}. \tag{23}$$

In the limit $y \to \infty$, we again seek a solution for which $yf \to$ constant, and as in Section 2 for the case $k = 0$, we see that if such a solution exists, then $yf \to 3$. In this case the terms Le^{-2y} and $-\frac{1}{3}kf^3e^{-3y}$ are exponentially small in this limit, and can be neglected. Hence, using the transformation (9) we again obtain (10) and the argument in Section 2 for the case $k = 0$ can be repeated here. We conclude that there is a unique solution such that $\psi \to \infty$, $R \to 0$ where asymptotic behaviour is given by (18). We shall again call this the barrier orbit, but the crucial question now is whether or not the barrier orbit is such that $\psi \to 0$ as $R \to R_c$.

First, let $0 < L < L_0$, when the turning-point curve (19) belongs to case (b) (see Figure 6(b)) for all $k > 0$. Hence the unique orbit defined by the asymptotic behaviour (18), while commencing in a region where $d\psi/dR$ is negative, must cross

https://doi.org/10.1017/S0334270000010195 Published online by Cambridge University Press

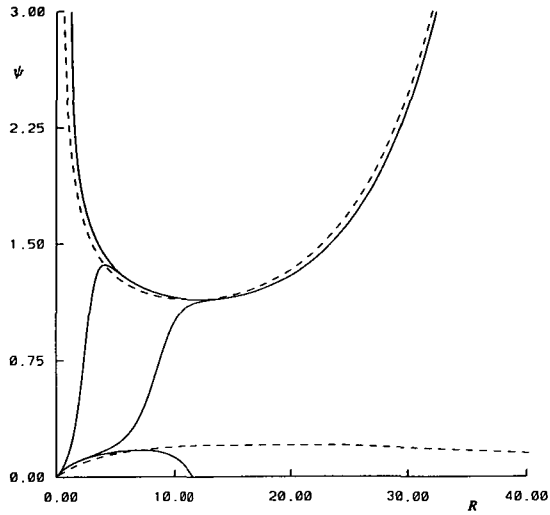

FIGURE 7. Typical orbits when $k = 0.0001$ and $L = 0.1$ $(0 < L < L_0)$. The dashed curves are the turning-point curves.

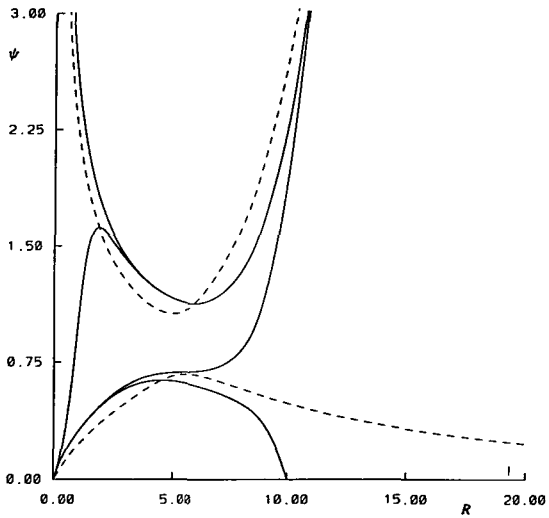

FIGURE 8. Typical orbits when $k = 0.003$ $(k > k_c)$ and $L = 0.5$ $(L > L_0)$. The dashed curves are the turning-point curves.

https://doi.org/10.1017/S0334270000010195 Published online by Cambridge University Press

the upper branch of the turning-point curve, and hence enter a region where $d\psi/dR$ is positive. The orbit then remains in this region, and passes to infinity. Crucial to this conclusion is the observation that the maximum point on the lower-branch of the turning-point curve (18) always lies below and to the right of the minimum point on the upper branch. Indeed these two points both lie on the curve $k\psi R^4 = 2$, which has ψ monotonically decreasing as R increases. We also note that any orbit crossing from a region where $d\psi/dR$ is positive to a region where $d\psi/dR$ is negative must do so to the left of the maximum (minimum) point on the lower branch (upper branch) of the turning-point curve (19). Similarly any orbit crossing from a region where $d\psi/dR$ is negative to a region where $d\psi/dR$ is positive must be to the right of the same maximum (minimum) point. Thus we can conclude that for the family of orbits emerging from the origin, defined by the parameter A (see (6)), there is a critical value of A, A_c, such that for $A > A_c$ the orbit emerges from the origin and passes to infinity with the asymptotic behaviour (20a). For A sufficiently large these orbits will cross the upper branch of the turning-point curve (19) twice, but of course will remain below the barrier orbit. For $A < A_c$ the orbit emerges from the origin, crosses the lower branch of the turning-point curve (19) and then $\psi \to 0$ as $R \to R_0$, where $0 < R_0 < \infty$ with $R_0 \to \infty$ as $A \to A_c$ from below. The situation is sketched in Figure 7.

Next, we let $L > L_0$ but suppose that $k > k_c$, so that the turning-point curve is again described by Figure 6(b). The conclusions here are now similar to those of the preceding paragraph. That is, the barrier orbit passes to infinity, and of the orbits emerging from the origin, either, for $A > A_c$ they likewise pass to infinity, or for $A < A_c$, $\psi \to 0$ as $R \to R_0$. A typical situation is sketched in Figure 8.

Finally, we let $L > L_0$ but suppose that $0 < k < k_c$, so that the turning-point curve (19) is described by Figure 6(a). Now the barrier orbit has the possibility to remain in the region where $d\psi/dR$ is negative, and hence $\psi \to 0$ as $R \to R_c$. We find that this will occur for $0 < k < k_0$ where $k_0 < k_c$. In this situation all the orbits emerging from the origin will cross the left-hand branch of the turning-point curve, and then as $t \to \infty$, $\psi \to 0$ as $R \to R_0$ where $0 < R_0 < R_c$. Some typical orbits are sketched in Figure 9(a). However, for $k_0 < k < k_c$, the barrier orbit crosses the right-hand branch of the turning-point curve, and then passes to infinity. This case is generally similar to that for $k > k_c$ described in the previous paragraph, and the orbits emerging from the origin either pass to infinity for $A > A_c$, or for $A < A_c$, $\psi \to 0$ as $R \to R_0$. Some typical orbits are sketched in Figure 9(b). Thus for $L > L_0$ it is k_0 which is the crucial value of k, rather than k_c. It is determined by the fate of the barrier orbit as R increases. Some typical values of k_0 as a function of L are shown in Table 3. Finally we note that since the orbits which pass to infinity do so with the asymptotic behaviour (20a), it follows from (1a) that they reach infinity in finite time.

(a)

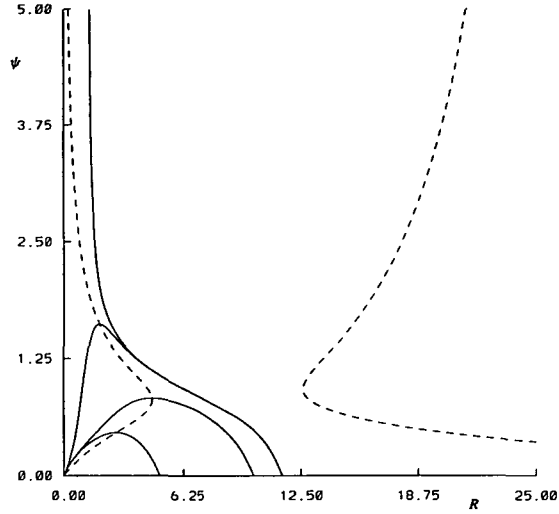

(b)

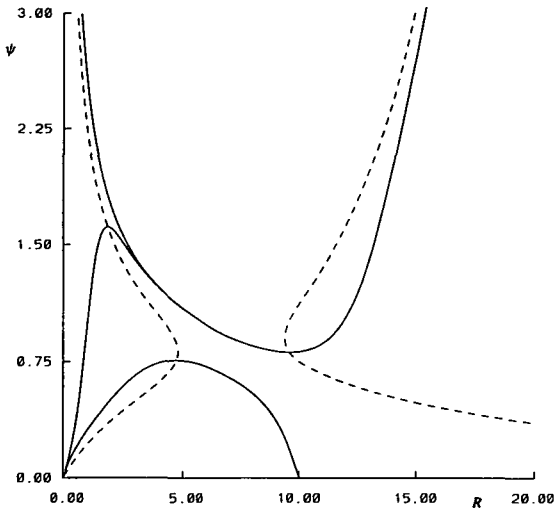

FIGURE 9. Typical orbits when $L = 0.5$ ($L > L_0$) and (a) $k = 0.0005$ ($0 < k < k_0$), or (b) $k = 0.001$ ($k_0 < k < k_c$). The dashed curves are the turning-point curves.

L	k_0
0.3	0.000029
0.5	0.00082
0.7	0.0037
0.9	0.009935

TABLE 3. The values of k_0 in terms of L.

https://doi.org/10.1017/S0334270000010195 Published online by Cambridge University Press

4. Summary

In this paper we have described analytical and numerical results for (2), which arises as a model for an expanding spherical flame front in a zero-gravity environment. Equation (2) determines the flame front speed as function of the radius. The corresponding behaviour in time can be deduced from (1a, b). Our emphasis has been on the behaviour of solutions for small values of the parameter k.

The key component in the interpretation of our results is the existence of a barrier orbit, which is defined as the unique orbit such that $\psi \to \infty$ as $R \to 0$, where it has the asymptotic behaviour (18). The central question is then whether or not the barrier orbit extends down to the limit $\psi \to 0$, $R \to R_c$. In the former case, it acts as a true barrier, and all orbits emerging from the origin must quench, that is $\psi \to 0$ as $r \to R_0$ for $0 < R_0 < R_c$ as $t \to \infty$. Otherwise the barrier orbit will pass to infinity, and orbits emerging from the origin will either quench or likewise pass to infinity.

We find that for $0 \leq k < k_0$ and $L > L_0$ (where $L_0 = 1/2e$), the barrier orbit is a true barrier in the sense described above, and all orbits emerging from the origin extinguish. Here k_0 depends on L, while R_c depends on both k and L. For $L > L_0$ but close to L_0, we find that k_0 is quite small, and since $R_c \to \infty$ as $k \to k_0$, the solutions exhibit some sensitivity to the actual value of k.

For $k > k_0$ and $L > L_0$, the barrier orbit passes to infinity and is not a true barrier. This also occurs for all $k > 0$ when $0 < L < L_0$. In these cases the solutions emanating from the origin either quench, or pass to infinity, depending on whether $A < A_c$ or $A > A_c$ respectively, where A is defined by the limiting behaviour as $\psi, R \to 0$ (see (6)). Since A defines the initial curvature, whereas numerically defined initial conditions near $\psi = R = 0$ define only the initial slope, the orbits emerging from the origin exhibit numerical sensitivity to the numerical initial conditions, particularly evident when $k > k_0$ and $L > L_0$ for k close to k_0. Indeed, there is a tendency for orbits emerging from the origin to approach the barrier orbit and apparently follow it quite closely for a while. Finally we note that when $k = 0$ and $0 < L < L_0$ the orbits either quench, or pass to infinity as a steadily propagating flame front (i.e. $\psi \to \psi_0^+$ as $R \to \infty$). However, for any $k > 0$, there can be no steadily propagating flame fronts and orbits which pass to infinity do so as $\psi, R \to \infty$.

Acknowledgements

The authors are grateful to Professor J.D. Buckmaster, who drew their attention to the interesting behaviour of the solutions of (2).

References

[1] J. Buckmaster and C. J. Lee, "The effects of confinement and heat loss on outwardly propagating spherical flames", 1992, preprint.

[2] P. D. Ronney and G. I. Sivashinsky, "A theoretical study of propagation and extinction of nonsteady spherical flame fronts", *SIAM J. Appl. Math.* **49** (1989) 1029–1046.

https://doi.org/10.1017/S0334270000010195 Published online by Cambridge University Press